Supplementary Information for

Redox and structural stability for sodium-ion batteries through bond structure engineering

Xingyu Li[1,2], Yi Li[1,2], Qinwen Cui[1,2], Minghui Zhong[1,2], Xiaolin Zhao[1,2*] and Jianjun Liu[1,2,3*]

[1]State Key Laboratory of High Performance Ceramics and Superfine Microstructure, Shanghai Institute of Ceramics, Chinese Academy of Sciences, 1295 Dingxi Road, Shanghai 200050, China

[2]Center of Materials Science and Optoelectronics Engineering, University of Chinese Academy of Sciences, Beijing 100049, China

[3]School of Chemistry and Materials Science, Hangzhou Institute for Advanced Study, University of Chinese Academy of Sciences, 1 Sub-lane Xiangshan, Hangzhou 310024, China

*Email: jliu@mail.sic.ac.cn; zhaoxiaolin@mail.sic.ac.cn

Experimental Section

Synthesis: O3-$NaNi_{0.2}Fe_{0.2}Mn_{0.6}O_2$ and O3-$NaNi_{0.2}Fe_{0.2}Mn_{0.3}Mg_{0.1}Cu_{0.1}Sn_{0.1}O_2$ were both synthesized through conventional solid-state sintering. Na_2CO_3 (5wt% excess), NiO, Fe_2O_3, Mn_2O_3, MgO, CuO and SnO_2 were weighed according to the stoichiometric ratio, and then mixed in a ball mill at a rotating speed of 35 rpm for 8 h. After the milling process, the mixture was pressed into pieces and calcined at 950 °C for 15 h in the muffle furnace. After natural cooling to room temperature, the samples were stored in an Argon-filled glovebox for protection.

The configurational entropy can be calculated by the equation:

$$\Delta S_{config} = -R\left[\left(\sum_{i=1}^{N} x_i ln x_i\right)_{cationsite} + \left(\sum_{j=1}^{M} x_j ln x_j\right)_{anionsite}\right] \quad \text{(Equation S1)}$$

where R is the universal gas constant, M and N are the numbers of cationic and anionic elements, x_i and x_j represent the ionic mole fractions of the cationic and anionic sites, respectively.

Electrochemical Tests: The synthesized active material, Super P carbon black and polyvinylidene fluoride (PVDF) binder are uniformly mixed in a mass ratio of 8:1:1 in N-methyl-2-pyrrolidone (NMP) solvent. The paste was uniformly applied to the aluminum foil and dried overnight in a vacuum oven before being cut into 14 mm diameter electrode sheets. The electrode tabs were encapsulated with sodium metal in 2032-type coin cells to form a half-cell for subsequent electrochemical performance testing. The glass fiber film was used as the separator, and the electrolyte is 1M NaClO4 dissolved in ethylene carbonate/diethyl carbonate (EC/DEC, 1:1, v/v) with 5% fluoroethylene carbonate (FEC). Electrochemical performance testing is carried out on

a battery test system (CT-3002A, LAND), and impedance testing is conducted on an electrochemical workstation (Metrohm-Autolab, PGSTAT 302N). Galvanostatic intermittent titration technique (GITT) is measured by applying the repeated current pulses for 20 min at a current density of 0.1C followed by relaxation for 3h.

Calculation of Na+ diffusion coefficient from GITT results:

$$D_{Na^+} = \frac{4}{\pi\tau}\left(\frac{m_B V_M}{M_B S}\right)^2\left(\frac{\Delta E_S}{\Delta E_\tau}\right)^2 \left(\tau \ll \frac{L^2}{D}\right) \quad \text{(Equation S2)}$$

where m_B is the mass of the active material in the electrode, V_M is the molar volume, M_B is the molecular weight of the material, S is the active surface area between the electrolyte and the electrode, ΔE_S is the steady state voltage difference of the cell, ΔE_τ is the total transient voltage difference of the cell when the current is applied for a time τ, τ is the duration of the applied current, and L is the diffusion distance of Na^+ from the lattice to the liquid electrolyte.

Material Characterizations: In-situ X-ray diffraction patterns (XRD) data of the electrode material was obtained using Cu Kα radiation on D8 ADVANCE in the range from 10° to 50° with a scan speed of 2° min^{-1}. By using the GSAS-II software, the XRD Rietveld refinement can be obtained for the analysis of crystal structure. Scanning electron microscopy (SEM) measurements were collected using Verios G4. High-resolution transmission electron microscopy (HR-TEM) images and energy dispersive X-ray spectroscopy (EDS) mappings were performed on a JEM 2100F microscope. The elemental content of the materials was obtained by ICP-OES test (PerkinElmer ICP 2100). The valence change of the element in different states is detected by X-ray photoelectron spectroscope (XPS, Thermo Kalpha).

Computational Details: Vienna ab initio Simulation Package (VASP) was employed to perform DFT calculations.[1] The Perdew–Burke–Ernzerhof (PBE) exchange-correlation function of the generalized gradient approximation (GGA) was used to describe the electron exchange-correlation energy.[2] The Hubbard U correction was adopted to correct electron-electron interactions (the U parameter of Ni 3d, Fe 3d, Mn 3d, Cu 3d and Sn were 6.2, 5.3, 3.9, 7.2 and 4.4 eV, respectively).[3] Besides, the projector-augmented-wave method (PAW) with the cut-off energy of 520 eV. The *k*-point sampling of the Monkhorst–Pack scheme was a 2×6×2 grid.[4] The electronic energy convergence criterion and atomic forces were set as 10^{-5} eV and 0.01 eV $Å^{-1}$. The supercell program was used to perform sampling of structures with different sodium content during the desaturation process. The bond valence site energy (BVSE) calculations based on SoftBV software tool were performed to investigate the diffusion pathways and the migration energy barriers of sodium ion.[5]

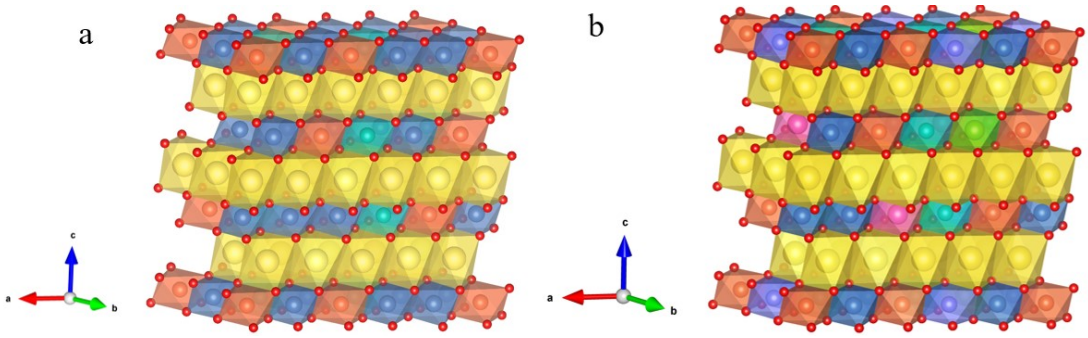

Fig.S1 The crystal structures of (a) NFM and (b) HE materials.

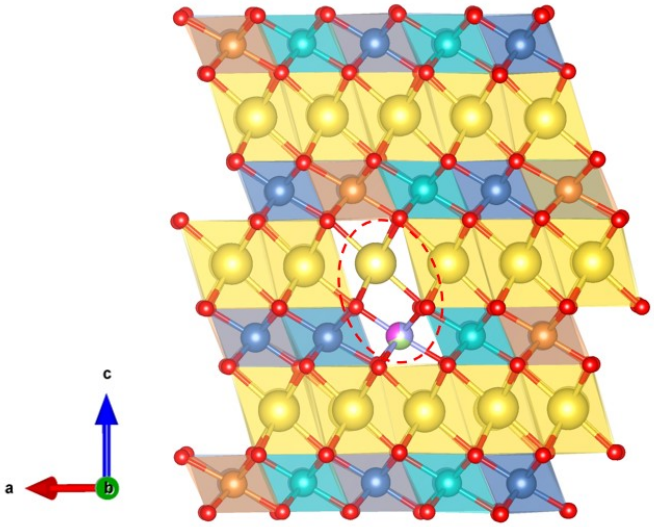

Fig.S2 The structure of the NFM for calculations and the corresponding Na-O-TM configuration.

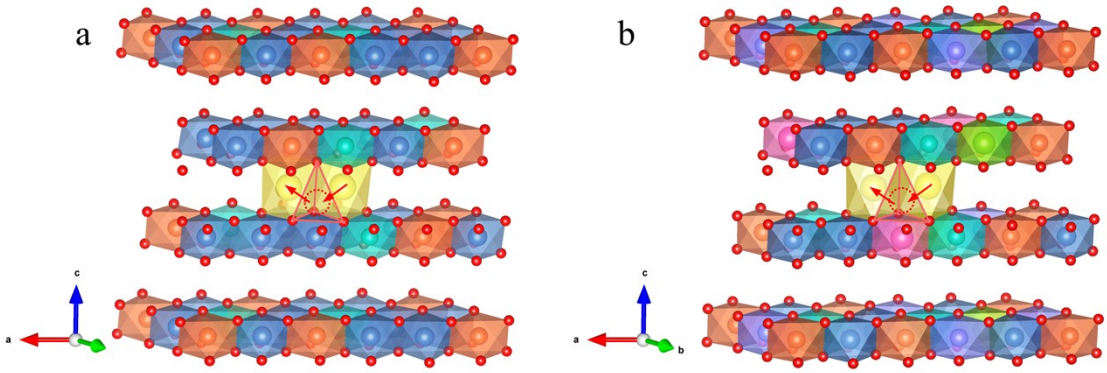

Fig.S3 The sodium ion migration pathway diagrams of (a) NFM and (b) HE materials.

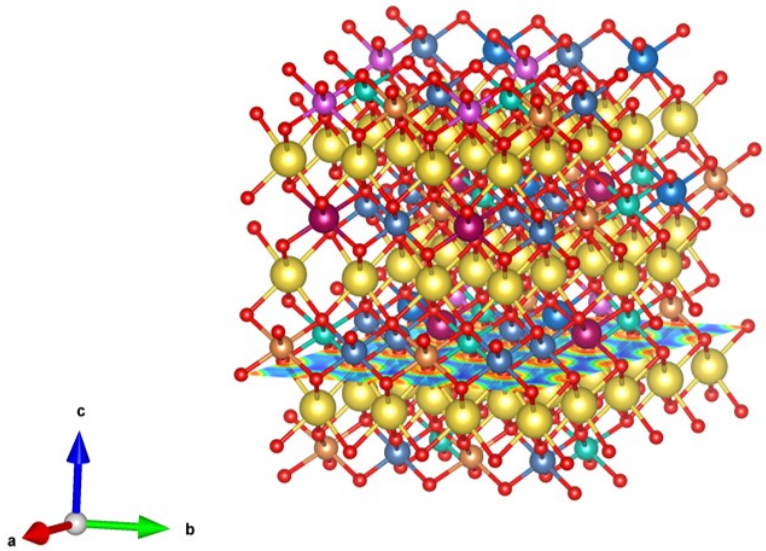

Fig.S4 The crystal structure of HE cathode materials sliced along the (001) lattice plane.

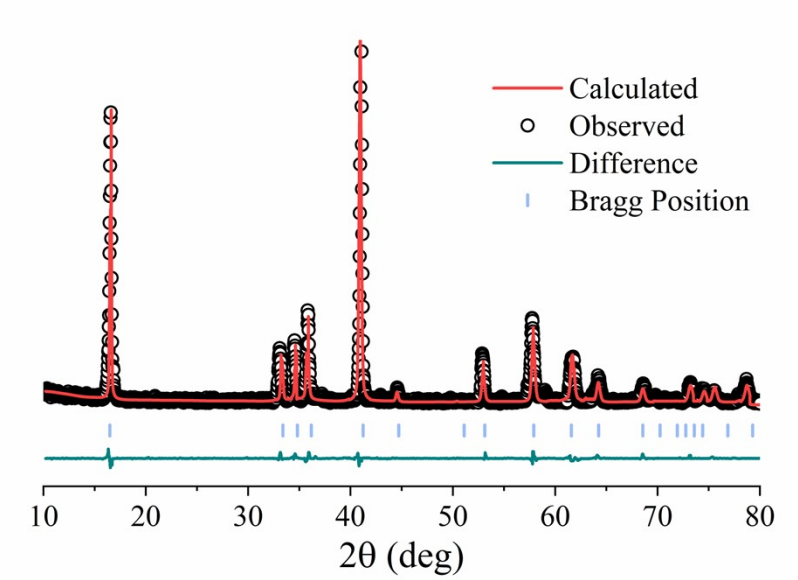

Fig.S5 The refined XRD results of NFM and the standard card of O3 phase structure.

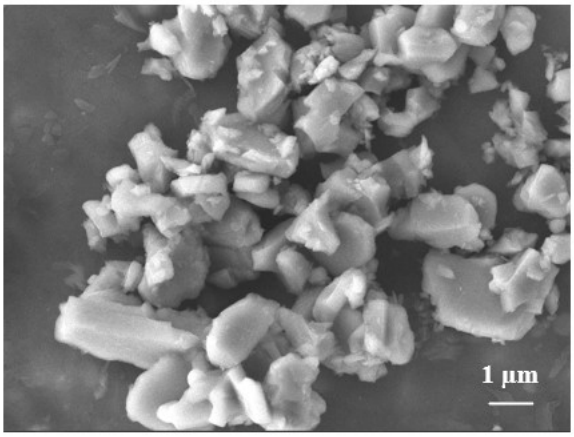

Fig.S6 SEM images of NFM. Electrode material morphology tends to be in the form of lumps.

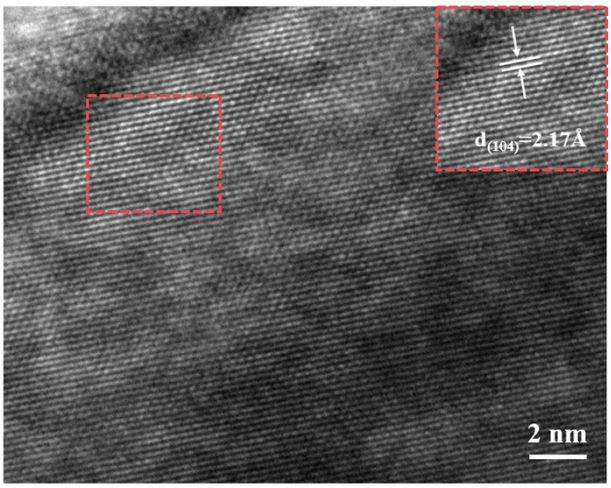

Fig.S7 HRTEM image of NFM and the $d_{(104)}$ interlayer distance is 2.17Å.

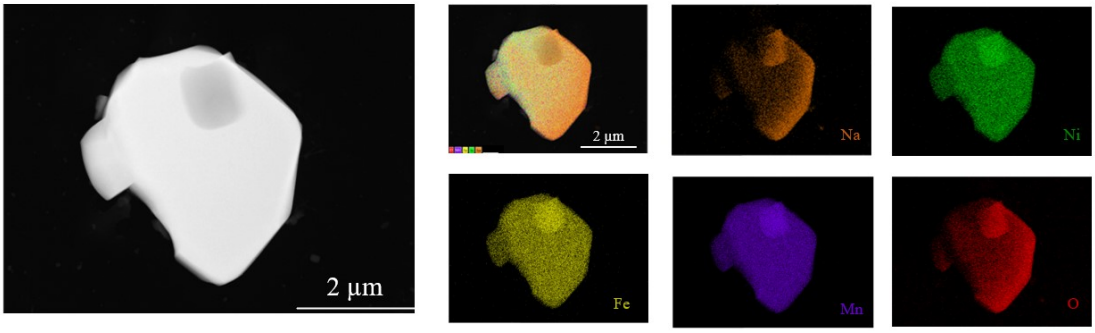

Fig.S8 EDS mappings of NFM. The Na, Ni, Fe, Mn and O elements are uniformly distributed in the sample.

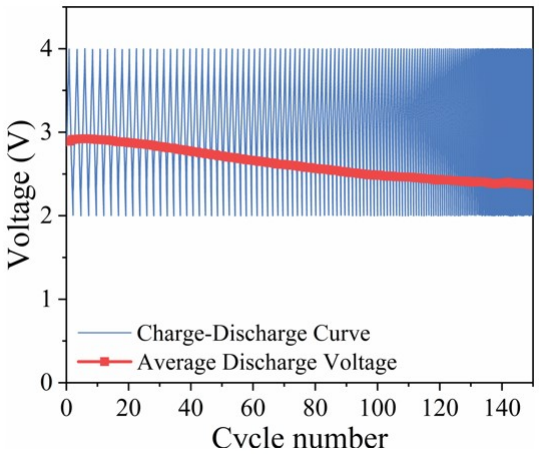

Fig.S9 The average discharge voltage variation of NFM electrode materials in the voltage range of 2-4 V at 0.3C current density.

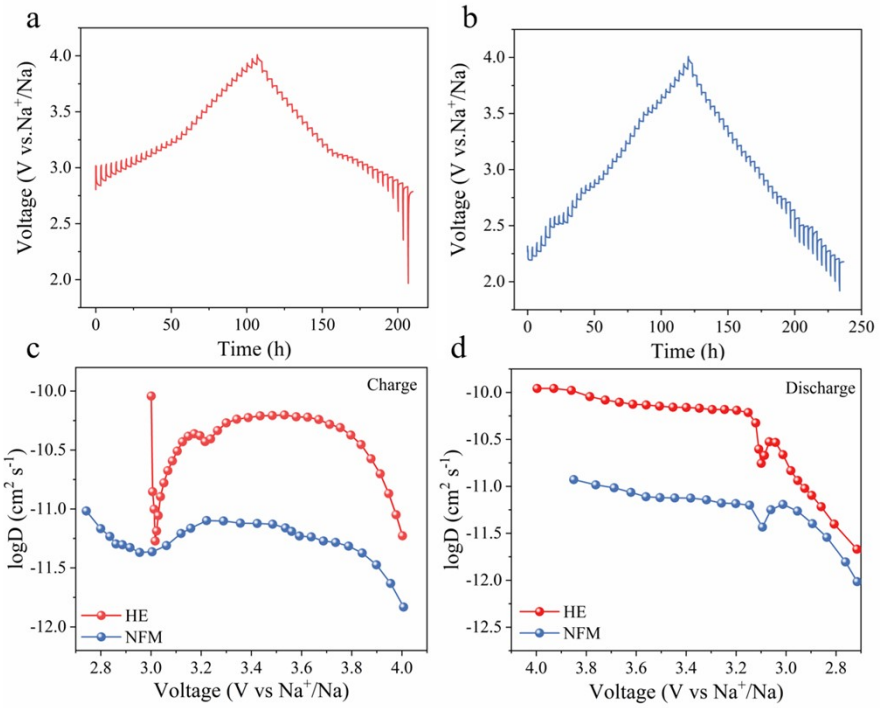

Fig.S10 The first lap GITT curves for (a) HE and (b) NFM. (c-d) Na^+ diffusion coefficients during the charge and discharge processes based on GITT tests.

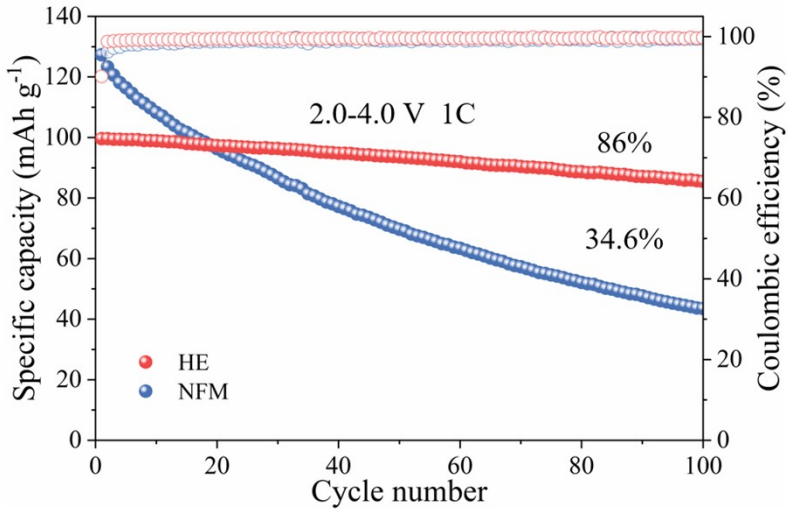

Fig.S11 The electrochemical cycling of HE and NFM at 1C current density.

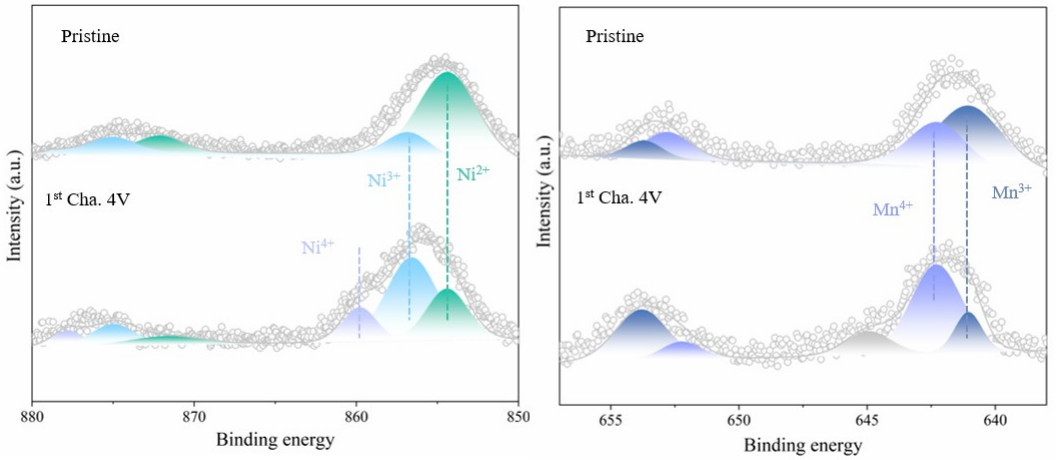

Fig.S12 The variation of Ni and Mn core spectra in NFM during the charging process, where the oxidization process of $Ni^{2+/3+/4+}$ and $Mn^{3+/4+}$ are the main sources of capacity, which provide 35% and 65% of the capacity, respectively.

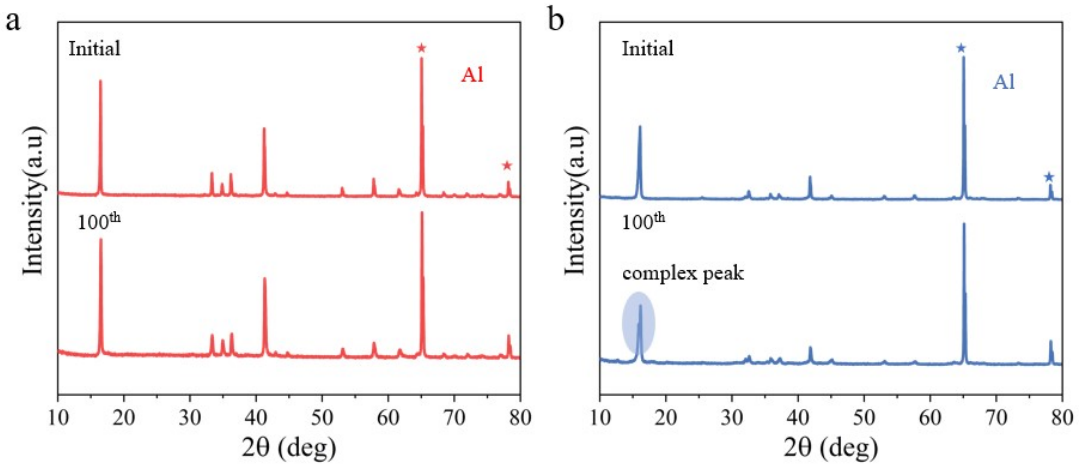

Fig.S13 Evolution of XRD patterns of (a) HE and (b) NFM cathode after 100 cycles at 5C current density. The XRD of HE remained unchanged. In contrast, the main peak (003) of NFM showed a composite peak.

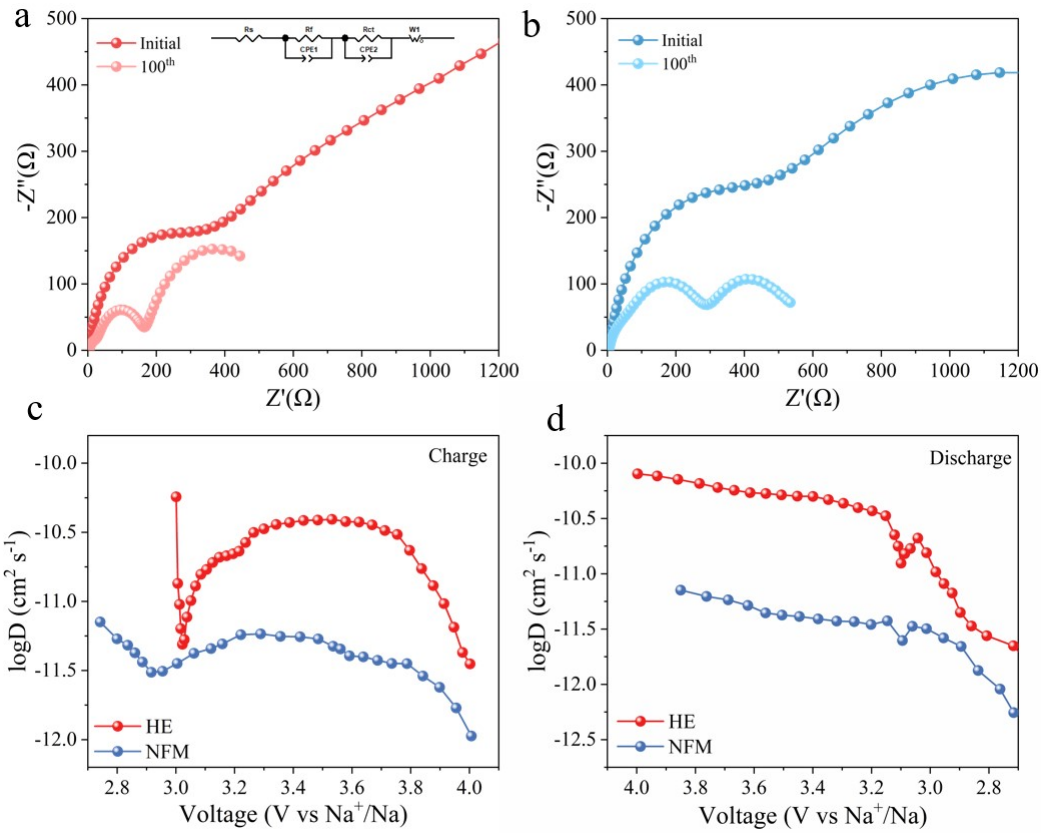

Fig.S14 The change in impedance spectra of electrodes before and after cycles (the inset is the equivalent circuit). (a-b) The resistance of the HE was gradually reduced from 545 to 172 Ω, while the resistance of the NMMO was only reduced from 707 to 316 Ω. (c-d) The sodium ion diffusion coefficient after ten cycles of the GITT test.

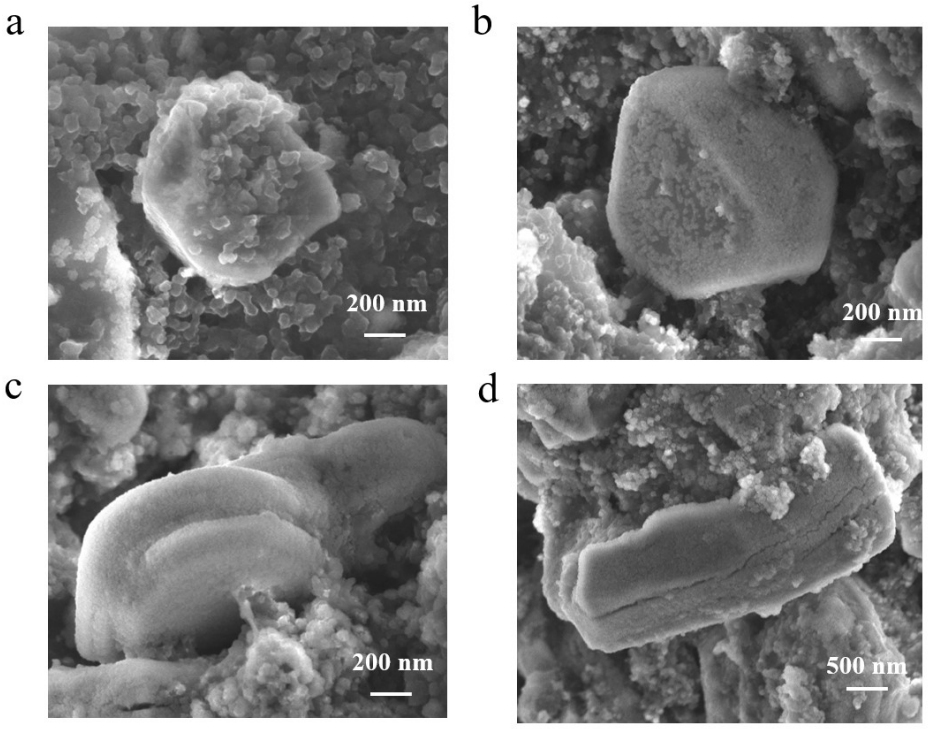

Fig.S15 SEM images of (a, b) HE and (c, d) NMMO after 100 cycles. The HE still maintained the intact particles, while the NFM showed a serious cracking.

Table S1. Lattice parameters of HE cathode material derived from Rietveld refinement

atom	site	x	y	z	occ.
Na	3a	0	0	0	1
Ni	3b	0	0	0.5	0.2
Fe	3b	0	0	0.5	0.2
Mn	3b	0	0	0.5	0.3
Mg	3b	0	0	0.5	0.1
Cu	3b	0	0	0.5	0.1
Sn	3b	0	0	0.5	0.1
O	6c	0	0	0.2335	1
$R\bar{3}m$.	a=3.0059Å	c= 16.0502 Å	V= 125.5940 Å^3		Rwp: 8.92

Table S2. Lattice parameters of NFM cathode material derived from Rietveld refinement

atom	site	x	y	z	occ.
Na	3a	0	0	0	1
Ni	3b	0	0	0.5	0.2
Fe	3b	0	0	0.5	0.2
Mn	3b	0	0	0.5	0.6
O	6c	0	0	0.2335	1
$R\bar{3}m$.	a=2.9714Å	c= 16.0152 Å	V= 123.8817 Å^3		Rwp: 9.61

Table S3. ICP-OES results of NFM and HE materials

Sample	Measured atomic ration						
	Na	Ni	Fe	Mn	Mg	Cu	Sn
NFM	1	0.2	0.2	0.6	0	0	0
HE	1	0.2	0.2	0.3	0.1	0.1	0.1

Table S4. Parameter table for button cell batteries

Materials	Cathodes' mass loading (mg)	Electrolyte amount (μl)	Radius (mm)	Thicknesses (μm)
HE	**3.5**	**150**	**14**	**20**
NFM	**3.6**	**150**	**14**	**20**

References

1. G. Kresse and J. Furthmüller, *Computational Materials Science*, 1996, **6**, 15-50.
2. J. P. Perdew, K. Burke and M. Ernzerhof, *Physical Review Letters*, 1996, **77**, 3865-3868.
3. A. Jain, G. Hautier, S. P. Ong, C. J. Moore, C. C. Fischer, K. A. Persson and G. Ceder, *Physical Review B*, 2011, **84**, 045115.
4. H. J. Monkhorst and J. D. Pack, *Physical Review B*, 1976, **13**, 5188-5192.
5. H. Chen and S. Adams, *IUCrJ*, 2017, **4**, 614-625.